

Hydrothermally synthesized nanocrystalline Nb₂O₅ and its visible-light photocatalytic activity for the degradation of congo red and methylene blue

Subhash Dharmraj Khairnar, Manohar Rajendra Patil, Vinod Shankar Shrivastava*

Nano-Chemistry Research Laboratory, G. T. Patil College, Nandurbar-425412 (M.S), India.

Received 1 December 2017; received in revised form 24 April 2018; accepted 30 April 2018

ABSTRACT

Nb₂O₅ nanoparticles were synthesized by the hydrothermal method. Structural, morphological and elemental analysis of synthesized Nb₂O₅ nanoparticles was carried out using X-ray diffraction (XRD), scanning electron microscopy (SEM) and energy dispersive X-ray spectroscopy, respectively. The average crystal size calculations were performed on the basis of X-ray diffraction pattern and were about 12.44 nm. The synthesized Nb₂O₅ nanoparticles were explored for the photocatalytic degradation of congo red (CR) and methylene blue (MB) dyes in their aqueous solutions using a spectrophotometric method. For the photocatalytic degradation of both the dyes, pH of dye solutions was varied in the range of 2 to 10. For the optimization, the maximum decolorization of 90 % and 87 % was observed for low initial dye concentration of 10 mg/L and pH values of CR and MB dyes were about 8 and 2, respectively. Besides, the effects of parameters such as the contact time and catalyst dose were studied systematically.

Keywords: Nb₂O₅, Hydrothermal method, Congo red, Methylene blue, Degradation, Pseudo first order.

1. Introduction

Nowadays, the world confronts so many environmental issues due to modernization and industrialization. However, both issues are responsible for water pollution, due to their carcinogenic behavior. The largest source of water pollution is untreated effluent containing organic dyes and pesticides engendered by industrial processes [1-5]. Besides, some of the dyes and pesticides contain a poisonous quality which has an impact on a variety of organs in human beings. Congo red (CR) is a diazo dye, most frequently used in industries. It contains the toxic substance which causes cancer in human beings [6-10]. Also, methylene blue (MB) is a heterocyclic aromatic chemical compound. The MB dye is stable and incompatible with the base. It may be noxious if it is inhaled and in contact with skin [5,11,12]. Thus, it is necessary to remove such hazardous materials from industrial effluent before they pollute the nearby fresh water streams. Environmental photochemistry utilizing nanocrystalline semiconducting material against the environmental

pollutions forms a component of the group of wastewater treatment method called Advanced Oxidation Processes (AOPs). AOPs are a group of processes that are predicated on the generation of hydroxyl radicals. These radicals are highly reactive, leading to the total mineralization of most of the organic pollutants [13]. Nanocrystalline materials mediated semiconducting photocatalysis is expeditiously becoming an efficient AOP, in which semiconductor material absorbs greater energy than its band gap energy which leads to the excitation of electrons from the valence band to the conduction band, consequently engendering electrons and holes. The valence band holes react with the water molecules and hydroxide ions to form hydroxyl radicals whereas the electron reacts with oxygen molecules and form superoxide radicals. These free radicals are extremely proficient oxidizers of organic dyes which can attack organic dyes and degrade them into CO₂ and H₂O [11,14]. In semiconductor photocatalyst, the excited electrons can easily move from the valence band to the conduction band at the same time; the holes migrate in the opposite direction. These transitions strongly prevent the recombination of the electron and hole and thereby increase the activity

*Corresponding author email: drvinod_shrivastava@yahoo.com
Tel.: +91 94 2390 5823; Fax: +91 25 6422 2293

of the photocatalyst [15-18]. Also, the nanocrystalline semiconducting material has higher surface area to volume ratio than its bulk. Thus this allows more preponderant photon absorption on the photocatalyst surface [19-24].

In recent years, for the removal of such inimical organic dyes and pesticides from industrial effluent by AOPs, nanocrystalline semiconductor material as a catalyst has been utilized. Niobium pentaoxide (Nb_2O_5) with the nanocrystalline size has gained much attention because of its physical, chemical, optical and electronic properties which make the Nb_2O_5 suitable for sundry catalytic applications [25-27], photocatalysis [28-30], sensors [31,32] and optical filters [33-35]. Up to now, several processes have been reported for the synthesis of Nb_2O_5 nano particles and thin films such as pulse laser decomposition [31], electro deposition [36], magnetron sputtering [37,38], plasma immersion ion implantation [39], the sol-gel process [40] and hydrothermal process [41].

The application of Nb_2O_5 as a catalyst for the photocatalytic degradation of dyes has been reported in the literature [42]. There are very limited studies on Nb_2O_5 photocatalyst used for the degradation of dyes. Therefore, the photocatalytic degradation of CR and MB by utilizing synthesized Nb_2O_5 photocatalyst under the visible-light irradiation is carried out in the present work. In this study the degradation of CR and MB from aqueous suspension was carried out. Both the CR and MB are extensively used and soluble in water also they are found to be potentially toxic, so it is necessary to remove such dyes from wastewater.

2. Experimental

2.1. Materials and methods

All chemicals and reagents used in this study are of the A.R grade. Commercial Niobium pentaoxide (Nb_2O_5) powder (99.9%), 25% Ammonia (NH_3), 30% Hydrogen peroxide (H_2O_2), sodium hydroxide (NaOH), ethylene glycol (EG), Methylene blue ($\text{C}_{16}\text{H}_{18}\text{ClN}_{13}\text{S}$) and Congo red ($\text{C}_{32}\text{H}_{22}\text{N}_6\text{Na}_2\text{O}_6\text{S}_2$) were purchased from S. D. Fine Chemicals, India and were used as received without further purification. The chemical structure of MB and CR is shown in Fig. 1S and 2S.

2.2. Preparation of dye solution

The stock solution (100 mg/L) of CR and MB was prepared using deionized water. The desired concentration of dye solutions (10, 20, 30, 40 and 50 mg/L) were prepared by diluting the stock solution with deionized water.

2.3. Synthesis of nano crystalline Nb_2O_5

The commercial Nb_2O_5 was taken and treated by the hydrothermal method to obtain nano particles of Nb_2O_5 . In a typical nanoparticles synthesis, 0.5 g Nb_2O_5 was mixed with 3 mL of 25% NH_3 and 40 mL of 30% H_2O_2 to give a clear homogeneous solution. Then 5 mL NaOH solution (0.4 M in EG) was added to provide a mild alkaline condition. The prepared solution was then transferred to a Teflon autoclave for 24 hours at 260 °C and cooled at room temperature. The white precipitate obtained was centrifuged to separate the powder from the liquid. The precipitate was washed a few times with deionized water and alcohol and dried at 60 °C for 5 hours in air. Finally, the precipitate was washed with deionized water and alcohol and calcinated at 500 °C for 2 hours. The nanoparticle synthesis procedure for the Nb_2O_5 is shown in Fig. 3S.

2.4. Characterizations

The synthesized nanocrystalline Nb_2O_5 was characterized by scanning electron microscopy (SEM-Hitachi S-4800 Japan), X-ray diffraction (XRD- Bruker D 8 Advance X-ray diffractometer Germany), electron dispersive X-ray spectroscopy (EDX- Bruker X Flash 5030) techniques and photocatalytic activity was performed by a UV-Vis spectrophotometer (Systronics 2203 India).

2.5. Photocatalytic degradation experiments

The photocatalytic degradation experiments were performed with a photocatalytic reactor. This bench scale framework contained a round and hollow Pyrex-glass cell with 1.0 L limit, 10 cm breadth and 15 cm stature. A 100 W mercury light was placed in a 5 cm width quartz tube with one end firmly fixed by a Teflon plug. The light and the tube were then submerged in the photoreactor cell with a light way of 3.0 cm. The entire reactor was cooled with a water-cooled and coated on its outside and the temperature was kept at 25 °C (Fig. 4S). All reactants in the reactions were stirred utilizing a magnetic stirrer to guarantee that the suspension of the catalyst was uniform over the span of the reactions. A cut off channel was connected to expel wavelengths underneath 420 nm to guarantee the contact of visible light. The photocatalytic activity of the catalyst was estimated by measuring the residual concentration of CR and MB in the solution. The spectrophotometric analysis of dyes before and after the irradiation was utilized to measure the decolorization efficiency of dyes. The absorbance of dyes was measured by using UV-Vis spectrophotometer at the wavelengths of absorbance maximum of dye (CR $\lambda_{\text{max}} = 497$ nm and MB $\lambda_{\text{max}} = 663$ nm). The decreasing absorbance of dye at the

wavelengths of absorbance maximum after the visible-light irradiation shows the decolorization rate of dye. The degradation efficiency of the dye has been calculated as shown in Eq. 1.

$$\% \text{ Degradation} = \frac{(C_0 - C_t)}{C_0} \times 100 \quad (1)$$

where C_0 is the initial dye concentration and C_t is the dye concentration after time t .

3. Results and Discussion

3.1. XRD analysis

The XRD analysis of Nb_2O_5 shown in Fig. 1 indicates the XRD pattern of Nb_2O_5 nanocrystals and the characteristic peaks of Nb_2O_5 nanocrystals are assigned and have good agreement with JCPDS card No. 30-0830. It shows the major diffraction peaks of 2θ at 46.61, 50.05, 53.38, 57.57 and 65.84. The high intensity of peaks indicates the crystalline nature of Nb_2O_5 . The structural parameters of Nb_2O_5 crystals are shown in Table 1S. The average crystalline size of Nb_2O_5 particles was estimated by the Scherer formula (Eq. 2) [43,44].

$$D = \frac{0.94 \lambda}{\beta \cos \theta} \quad (2)$$

where, D is the average crystalline size, λ is wavelength in angstrom, β is the FWHM in radian and θ is the diffraction angle in degree. The average crystalline size of Nb_2O_5 was found to be 12.44 nm.

3.2. SEM and EDX analysis

The EDX spectrum of modified Nb_2O_5 nanoparticles is shown in Fig. 2. It shows that the well-defined peaks

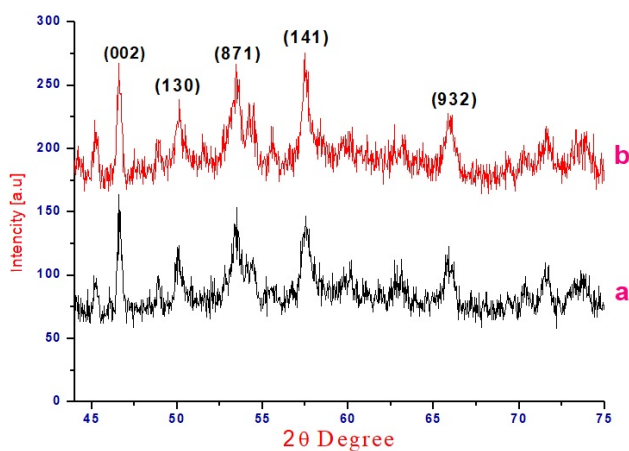


Fig. 1. XRD pattern of Nb_2O_5 nanoparticles (a) commercial Nb_2O_5 (b) modified Nb_2O_5 .

were related to Niobium and Oxygen and this clearly indicates that the synthesized nanocrystals are made of Nb and O. No other impurity was detected in the sample spectrum, which confirms the purity of the Niobium pentoxide. The exact amounts of specific elements including Niobium and Oxygen are 26.17%, 73.83% respectively. The SEM images of (Fig. 3) Nb_2O_5 show cubic morphology. The results suggest that the synthesized Nb_2O_5 nanoparticles are mesoporous and crystalline, and have rough surface area. Normally, a rough surface will be more photocatalytically active compared to smooth surfaces. A rough surface will display a higher surface area, leading to more photocatalytic sites, thus these microspores are sufficient to influence the photocatalytic activity of Nb_2O_5 nanoparticles. The particle size distribution of Nb_2O_5 catalyst estimated from SEM images is found to be very close to an average crystalline size calculated by XRD as shown in Fig. 4.

3.3. Photocatalytic studies

3.3.1. Effect of pH of solution

Effect of pH on the photocatalytic degradation of dyes was examined in the range of pH 2-10 in the presence of Nb_2O_5 photocatalyst for the contact time of 120 minutes at dyes concentration of 20 mg/L and catalyst dose of 1 gm/L as shown in Fig. 5, a and b. The pH is the most important parameter for controlling the photocatalytic degradation of dyes, especially due to its effect on the catalyst surface. The pH_{pzc} of the Nb_2O_5 catalyst was estimated at about 7.46 using reported method [45]. The surface has net zero charge at pH_{pzc} and at $\text{pH} < \text{pH}_{\text{pzc}}$ the surface of the catalyst is positively charged while at $\text{pH} > \text{pH}_{\text{pzc}}$ the surface is negatively charged.

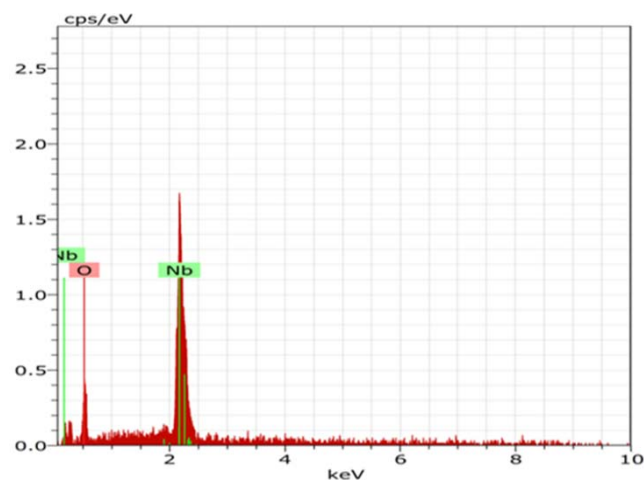


Fig. 2. EDX image of modified Nb_2O_5 nanoparticles.

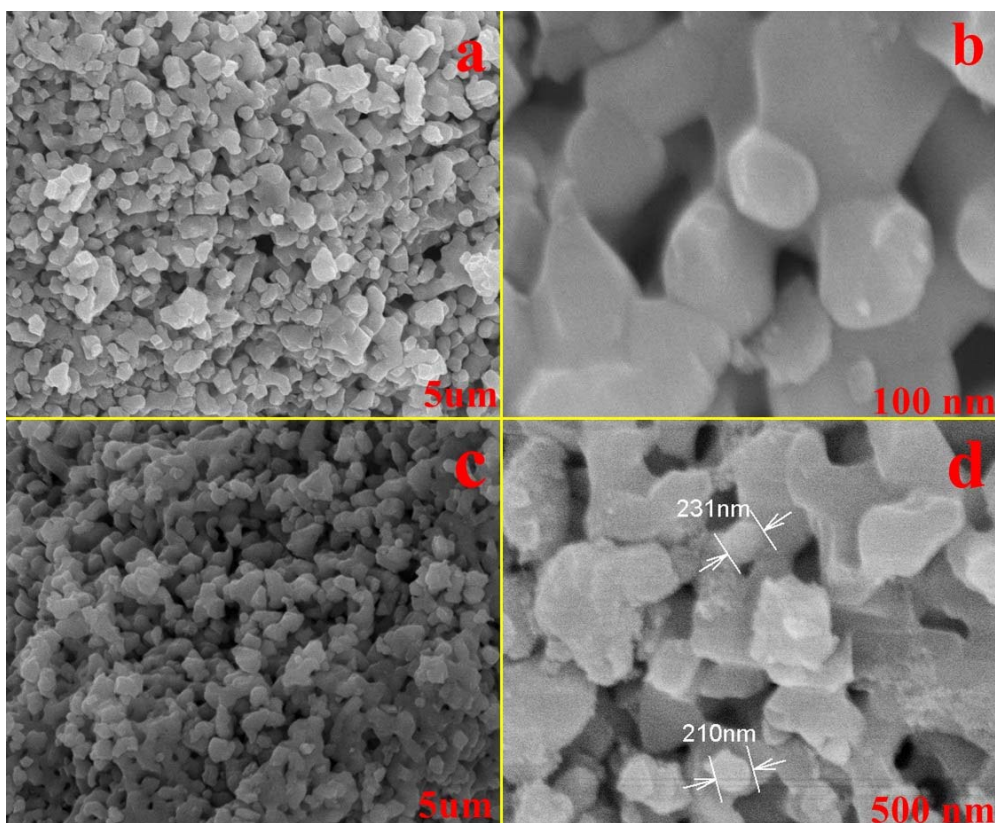


Fig. 3. SEM images of Nb₂O₅ nano particles (a, b, c) synthesized Nb₂O₅, (d) Commercial Nb₂O₅.

The maximum degradation of CR up to 80% was obtained at pH 8, the catalyst surface negatively charged in basic media. Therefore, a higher concentration of hydroxyl ion can be available to react with holes to form hydroxyl radical. The hydroxyl radicals are considered as the predominant species at higher pH. At higher pH, hydroxyl radicals are easily produced by oxidizing more and more hydroxide ions available on the Nb₂O₅ surface and thus the efficiency of the process is ultimately enhanced. But the degradation of CR was inhibited when the pH is high (pH > 8) because the hydroxyl ion competes with the CR molecules in the process of degradation on the surface of the Nb₂O₅ photocatalyst [46-49].

For MB, the maximum degradation up to 90 % was obtained at pH 2. The Nb₂O₅ surface is absolutely protonated at low pH and positively charged. At low pH, positive holes are major oxidizing species [47] and the catalyst photochemically acts as a photosensitizer. The redox potential of the photogenerated valence band holes is sufficiently positive to generate hydroxyl radicals. These radicals are responsible for the subsequent degradation of the MB dye. Also, these positive holes trap the MB dye; this leads to the direct oxidation of MB dye [50,51].

3.3.2. Effect of initial dye concentration:

The effect of initial dye concentration on the degradation efficiency was investigated at optimized pH (for CR, pH=8 and MB pH=2) by varying the initial dye concentration. Different initial concentrations of CR and MB with a range of 10-50 mg/L were used to evaluate the photocatalytic activity. Both dyes of CR and MB reveal the maximum degradation at initial dye concentration 10 mg/L shown in Fig. 6a and b.

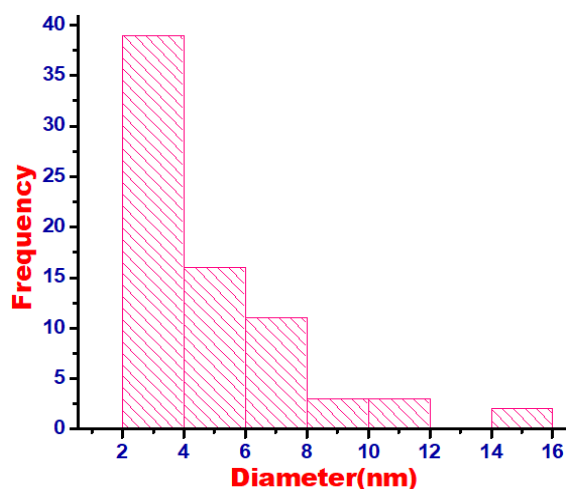


Fig. 4. The particle size distributions curve.

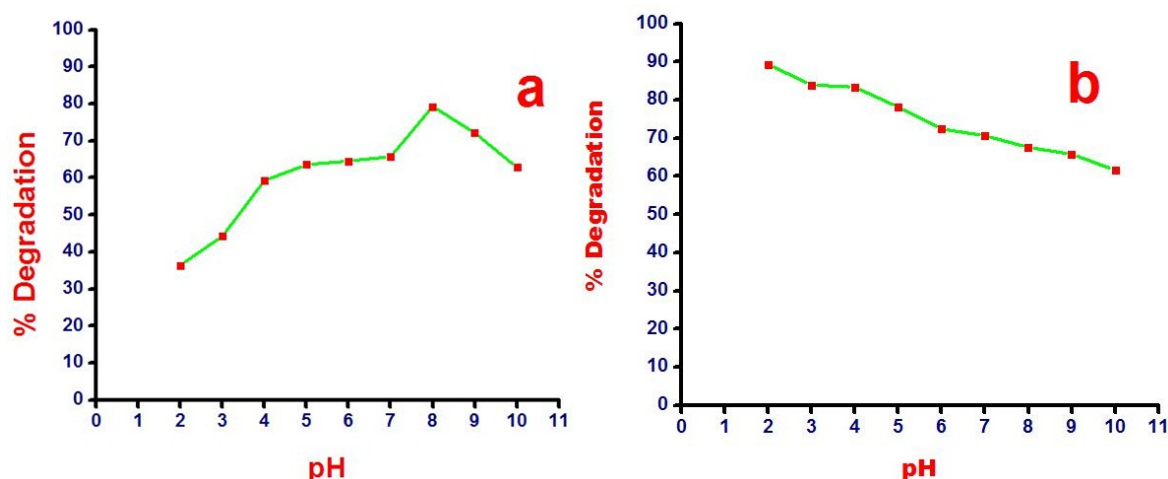


Fig. 5. Effect of pH on photocatalytic degradation of (a) CR conditions: pH= 2-10, dye concentration 20 mg/L and catalyst dose 1 gm/L for the irradiation time 120 min. (b) MB, conditions: pH= 2-10, dye concentration. 20 mg/L and catalyst dose 1 gm/L for the irradiation time 120 min.

The degradation efficiency of dyes (contact time of 120 minutes) decreased when the initial concentration of dyes increased. The efficiency of the catalyst decreased because the concentration of dyes increased. The excess of dye molecules will be adsorbed on the catalyst surface, so the active sites of the catalysts will be reduced. Therefore, with the increasing occupied space of catalyst surface by dye molecules, the hydroxyl radicals will be formed and they have a short lifetime to react with dye molecules. Further increase in dye concentration causes dye molecules to be absorbed on the photocatalyst surface and more number of hydroxyl radicals are required for the degradation of dye molecules.

On the other hand, the formation of hydroxyl radicals on the catalyst surface remains constant for a given light

intensity, catalyst dose and irradiation time. Hence hydroxyl radicals are insufficient for the degradation of dyes at high concentrations. Thus, photodegradation efficiency diminished [52,53].

3.3.3. Effect of contact time:

The effect of contact time on photocatalytic degradation of CR and MB dyes was studied at an optimum condition (for CR at pH 8 and for MB at pH 2) and dyes concentration of 10 mg/L. The fixed amount of Nb₂O₅ catalyst was 1 gm/L. The relationships between photocatalytic degradation of CR and MB dyes and the contact time were investigated. The results are shown in Fig. 7 (a) and (b). It can be seen that the degradation of CR and MB increases with an increase in the contact time [54].

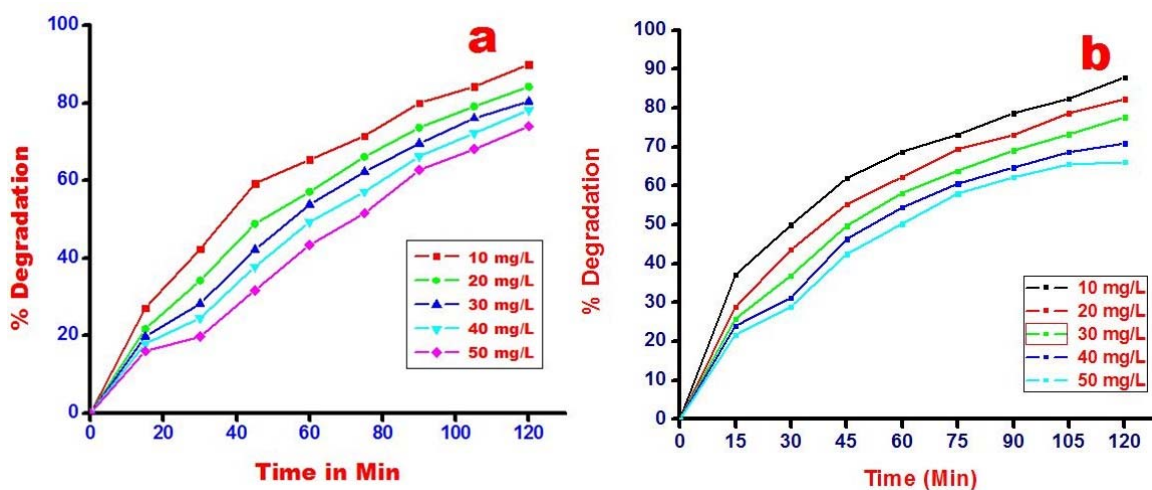


Fig. 6. Effect of initial dye concentration on the photocatalytic degradation (a) CR, conditions pH=8, dye concentration 10, 20, 30, 40, 50 mg/L and catalyst dose 1 gm/L for irradiation time 120 min. (b) MB, conditions: pH= 2 dye concentration 10, 20, 30, 40, 50 mg/L and catalyst dose 1 gm/L for irradiation time 120 min.

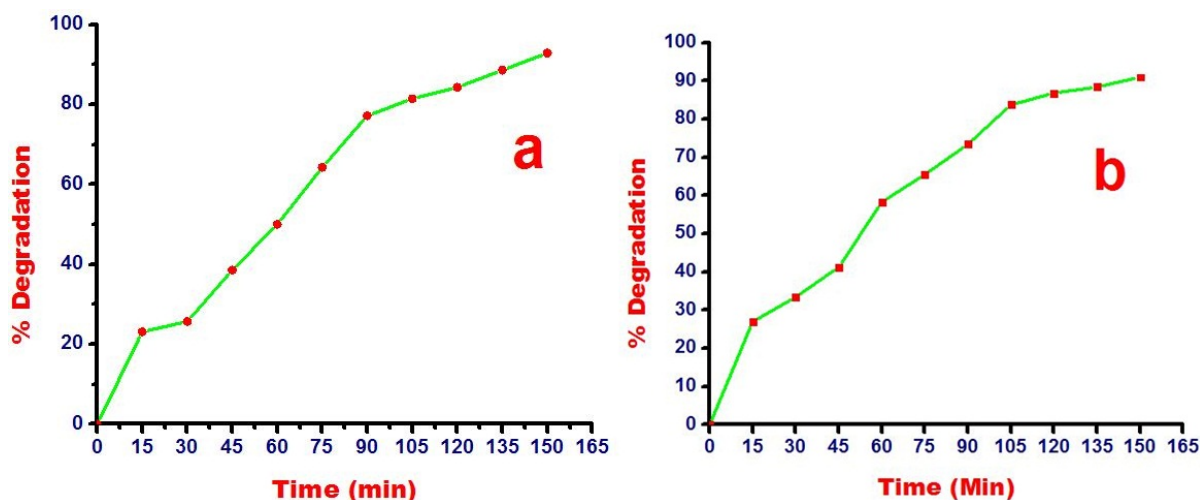


Fig. 7. Effect of contact time on photocatalytic degradation of (a) CR, conditions pH=8, dye concentration 10 mg/L and catalyst dose 1 gm/L irradiation time 120 min. (b) MB, conditions: pH= 2 dye concentration 10 mg/L and catalyst dose 1 gm/L irradiation time 120 min.

The rate of photocatalytic degradation is faster for first 90 minutes, and then it attains equilibrium. The faster photocatalytic degradation up to 90 minutes is due to the availability of a large number of active sites for photocatalytic degradation. Furthermore, between dye particles and catalyst surface there is repulsion which results in lowering of photocatalytic degradation rate.

3.3.4. Effect of catalyst dose:

The effect of photocatalyst dose was studied on dye degradation when other experimental conditions (for CR were at pH 8 and for MB at pH 2 and dyes concentration 10 mg/L for contact time 90 min) were constant. The degradation percentage of CR and MB by

Nb_2O_5 at different catalyst doses, 0.2–2 gm/L for 10 mg/L of dye concentration, was studied. It is observed that the rate of degradation initially increases with the increase in catalyst concentration and thereafter decreases as shown in Fig. 8 (a) and (b). Since the catalyst concentration increases, the agglomeration (particle-particle interaction) also increases, this is the major factor to reduce light absorption by the photocatalyst. Also, the agglomerations prevent photons reaching inner layers of the catalyst. Hence, the least amount of catalyst particles gets excited and ultimately less electron/holes and hydroxyl radical were produced. Therefore, the degradation rate tends to decrease as the catalyst dose increases [53].

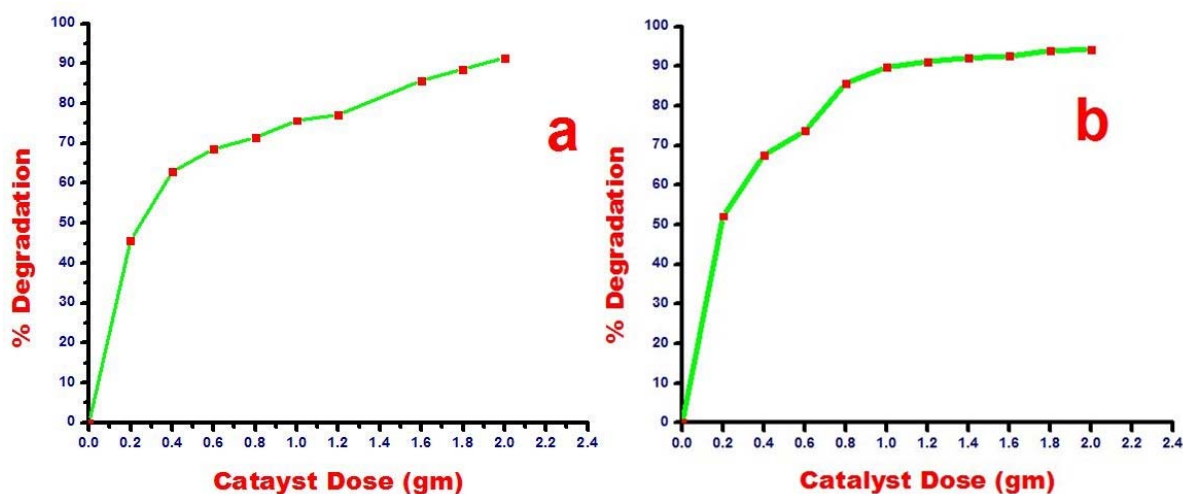


Fig. 8. Effect of catalyst dose on the photocatalytic degradation of (a) CR, conditions pH=8, dye concentration 10 mg/L and catalyst dose 0.2-2 gm/L irradiation time 90 min. (b) MB, conditions: pH= 2 dye concentration 10 mg/L and catalyst dose 0.2-2 gm/L irradiation time 90 min

3.5. Kinetics study

The photocatalytic degradation of CR and MB was found to be Pseudo-first order. It is seen that $\ln(C_0/C_t)$ is directly proportional to contact time. The photocatalytic degradation of CR and MB solution is directly proportional to concentration. So we can conclude that the photocatalytic degradation is the pseudo first order reaction. The apparent first-order kinetic equation of $\ln(C_0/C_t) = kt$ [55-56] was used to fit experimental data. Where k is the apparent rate constant, C_0 is the initial solution concentration of CR and MB, and C_t is the concentration of CR and MB at time t . The linear transform in $\ln(C_0/C_t)$ as a function of contact time is given in Fig. 9, a and b. This confirms that the kinetic curves were of apparent pseudo first-order. The slope of the $\ln C_0/C_t$ Vs time plot gives the value of the rate constant k in min^{-1} .

The photocatalytic activity can be compared to k value and linear regression coefficient (R^2) for CR and MB solution with different initial concentrations, these data are summarized in Table 1. The k values, which are obtained by linear fitting from Table 1 are 0.03915,

0.02763, 0.02303 min^{-1} for CR and 0.02533, 0.02993, 0.03684 min^{-1} for MB respectively.

4. Conclusions

Nb_2O_5 photocatalyst was synthesized and changed into nanoscale by the hydrothermal method. The crystallite size of the Nb_2O_5 photocatalyst was estimated to be about 12.44 nm. The degradation efficiency of the photocatalyst indicated that the low initial dye concentration and high catalyst dose are more favorable for the degradation process. The process obeys the pseudo first order kinetics with good correlation with linear regression coefficient. The experimental results of this study show that the Nb_2O_5 photocatalyst degrade CR and MB up to 90%. Therefore, Nb_2O_5 is a very promising catalyst for the degradation of dyes.

Acknowledgments

Authors gratefully acknowledge to North Maharashtra University, Jalgaon for providing financial support under the scheme of Shree G. H. Raisonni fellowship for doctoral research. Authors are thankful to DST-FIST for instruments.

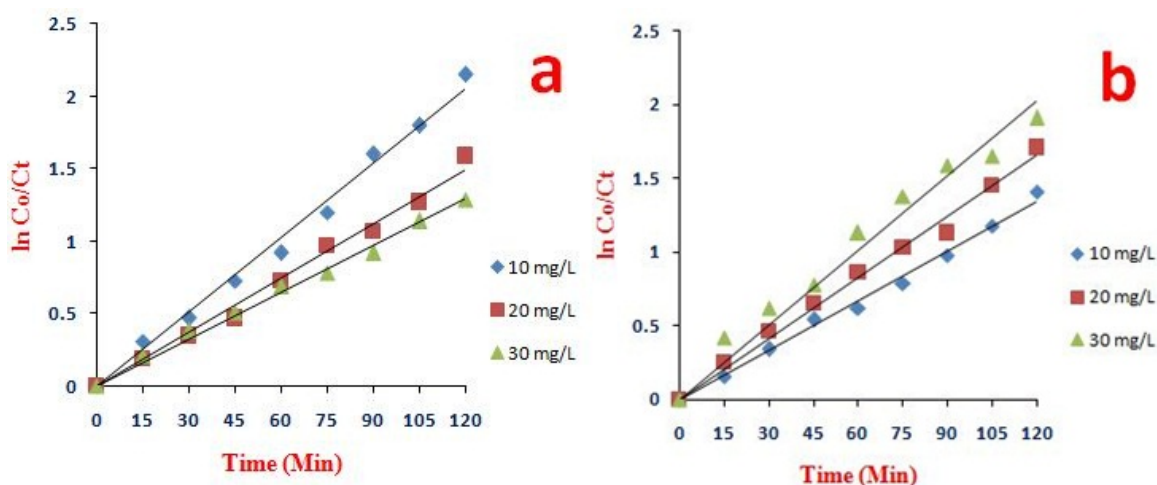


Fig. 9. Pseudo first order kinetics for photocatalytic degradation of (a) CR, conditions pH=8, dye concentration. 10, 20, 30 mg/L and catalyst dose 1 gm/L irradiation time 90 min. (b) MB, conditions: pH= 2 dye concentration. 10, 20, 30 mg/L and catalyst dose 1 gm/L irradiation time 90 min.

Table 1. Pseudo first order rate constant of CR and MB for Photocatalytic degradation.

Amount of catalyst in gm/L	Conc. of dye in gm/L		Rate Const.(K) min^{-1}		Linear regression coefficient (R^2)	
	CR	MB	CR	MB	CR	MB
1 gm/L	10	10	0.03915	0.02533	0.991	0.993
1 gm/L	20	20	0.02763	0.02993	0.989	0.991
1 gm/L	30	30	0.02303	0.03684	0.992	0.969

References

- [1] Y. He, *China Particuol.* 2 (2004) 168-170.
- [2] H. Chun, W. Yizhong, *Chemosphere* 39 (1999) 2107-2115.
- [3] J. Kiwi, C. Pulgarin, P. Peringer, M. Gratzel, *Appl. Catal. B.* 3 (1993) 85-99.
- [4] J. Li, Y. Xu, Y. Liu, D. Wu, Y. Sun, *China Particuol.* 2 (2004) 266-269.
- [5] H.R. Pouretedal, A. Norozi, M.H. Keshavarz, A. Semnani, *J. Hazard. Mater.* 162 (2009) 674-68.
- [6] M. Boeniger, Carcinogenicity and metabolism of azo dyes, especially those derived from benzidine, NIOSH Technical Report, 1980.
- [7] S. Maiti, S. Purakayastha, B. Ghosh, *Chem. Eng. Commun.* 195 (2007) 386-403.
- [8] S. Aghabeygi, R. K. Kojoori, H.V. Azad, *Iran. J. Catal.* 6 (2016) 275-279.
- [9] L. Shabani, H. Aliyan, *Iran. J. Catal.* 6 (2016) 221-228.
- [10] H.R. Pouretedal, M. Ahmadi, *Iran. J. Catal.* 3 (2013) 149-155.
- [11] A. Nezamzadeh-Ejhih, S. Hushmandrad, *Appl. Catal. A* 388 (2010) 149-159.
- [12] A. Buthiyappan, A. R. Aziz, W. M. Duad, *Rev. Chem. Eng.* 32 (2016) 1-47.
- [13] N.P. Mohabansi, V.B. Patil, N. Yenkie, *Rasayan J. Chem.* 4 (2011) 814-819.
- [14] M. Karimi-Shamsabadi, A. Nezamzadeh-Ejhih, *J. Mol. Catal. A: Chem.* 418-419 (2016) 103-114.
- [15] M.R. Hoffmann, S.T. Martin, W. Choi, D.W. Bahnemann, *Chem. Rev.* 95 (1995) 69-96.
- [16] T. Aarhi, P. Narahari, G. Madras, *J. Hazard. Mater.* 149 (2007) 725-734.
- [17] J. Esmaili-Hafshejani, A. Nezamzadeh-Ejhih, *J. Hazard. Mater.* 316 (2016) 194-203.
- [18] A. Nezamzadeh-Ejhih, Z. Ghanbari-Mobarakeh, *J. Ind. Eng. Chem.* 21 (2015) 668-676.
- [19] R.W. Matthews, *J. Catal.* 111 (1988) 264-272.
- [20] K. Dai, H. Chen, T. Peng, D. Ke, H. Yi, *Chemosphere.* 69 (2007) 1361-1367.
- [21] Z. Zainal, C.Y. Lee, M.Z. Hussein, A. Kassim, N.A. Yusof, *J. Hazard. Mater.* 118 (2005) 197-203.
- [22] S. Al-Qaradawi, S.R. Salman, *J. Photochem. Photobiol. A* 148 (2002) 161-168.
- [23] H. Kyung, J. Lee, W. Choi, *Environ. Sci. Technol.* 39 (2005) 2376-2382.
- [24] Y. Liu, X. Chen, J. Li, C. Burda, *Chemosphere* 61 (2005) 11-18.
- [25] M. Paulis, M. Martin, D.B. Soria, A. Diaz, J.A. Odriozola, M. Montes, *Appl. Catal. A.* 180 (1999) 411-420.
- [26] T. Ushikubo, *Catal. Today* 57 (2000) 331-338.
- [27] K. Nakajima, T. Fukui, H. Kato, M. Kitano, J.N. Kondo, S. Hayashi, M. Hara, *Chem. Mater.* 22 (2010) 3332-3339.
- [28] X. Chen, T. Yu, X. Fan, H. Zhang, Z. Li, J. Ye, Z. Zou, *Appl. Surf. Sci.* 253 (2007) 8500-8506.
- [29] J. Hwang, J. Kim, E. Ramasamy, W. Choi, J. Lee, *Microporous Mesoporous Mater.* 143 (2011) 149-156.
- [30] K. K. Behzad, A. F. Navid, H. Navid, *Int. J. Nano Dimens.* 8 (2017) 265-273.
- [31] M.E. Gimon-Kinsel, K.J. Balkus, *Microporous Mesoporous Mater.* 28 (1999) 113-123.
- [32] X. Xu, B. Tian, S. Zhang, J. Kong, D. Zhao, B. Liu, *Anal. Chim. Acta* 519 (2004) 31-38.
- [33] I. Sieber, H. Hildebrand, A. Friedrich, P. Schmuki, *Electrochem. Commun.* 7 (2005) 97-100.
- [34] N. Ozer, D.-G. Chen, C.M. Lampert, *Thin Solid Films* 277 (1996) 162-168.
- [35] P. Viswanathamurthi, N. Bhattarai, H.Y. Kim, D.R. Lee, S.R. Kim, M.A. Morris, *Chem. Phys. Letts.* 374 (2003) 79-84.
- [36] I. Zhitomirsky, *Mater. Lett.* 35 (1998) 188-193.
- [37] K. Yoshimura, T. Miki, S. Iwama, S. Tanemura, *Thin Solid Films* 281-282 (1996) 235-238.
- [38] F. Lai, M. Li, H. Wang, H. Hu, X. Wang, J.G. Hou, Y. Song, Y. Jiang, *Thin Solid Films* 488 (2005) 314-320.
- [39] W. Ensinger, J. Hartmann, H. Bender, R.W. Thoma, A. Koniger, B. Stritzker, B. Rauschenbach, *Surf. Coat. Technol.* 85 (1996) 80-85.
- [40] M. Macek, B. Orel, *Sol. Energy Mater. Sol. Cells.* 54 (1998) 121-130.
- [41] A. Khanfekr, M. Tamizifar, R. Naghizadeh, *Int. J. Nano Dimens.* 6 (2015) 277-281.
- [42] A.G.S. Prado, L.B. Bolzon, C.P. Pedroso, A.O. Moura, L.L. Costa, *Appl. Catal. B* 82 (2008) 219-224.
- [43] S. Aghdasi, M. Shokri, *Iran. J. Catal.* 6 (2016) 481-487.
- [44] H. Derikvandi, A. Nezamzadeh-Ejhih, *J. Photochem. Photobiol. A* 348 (2017) 68-78.
- [45] A. Nezamzadeh-Ejhih, M. Bahrami, *Desalin. Water Treat.* 55 (2015) 1096-1104.
- [46] M.A. Barakat, H. Schaeffer, G. Hayes, S. Ismat-Shah, *Appl. Catal. B* 57 (2005) 23-30.
- [47] U.G. Akpan, B.H. Hameed, *J. Hazard. Mater.* 170 (2009) 520-529.
- [48] A. Nezamzadeh-Ejhih, M. Karimi-Shamsabadi, *Chem. Eng. J.* 228 (2013) 631-641.
- [49] H. Derikvandi, A. Nezamzadeh-Ejhih, *J. Mol. Catal. A: Chem.* 426 (2017) 158-169.
- [50] K. Mahalik, J.N. Sahu, A.V. Patwardhan, B.C. Meikap, *J. Hazard. Mater.* 175 (2010) 629-637.
- [51] H. Haile, *Mod. Chem. Appl.* 4 (2016) 1-5.
- [52] C.-C. Wang, C.-K. Lee, M.-D. Lyu, L.-C. Juang, *Dyes Pigm.* 76 (2008) 817-824.
- [53] N. Ajoudanian, A. Nezamzadeh-Ejhih, *Mater. Sci. Semicond. Process* 36 (2015) 162-169.
- [54] Y.V. Marathe, M.M.V. Ramanna, V.S. Shrivastava, *Desalin. Water Treat.* 51 (2013) 5813-5820.
- [55] M.M. Sadiq, A.S. Nesaraj, *Iran. J. Catal.* 4 (2014) 219-226.
- [56] A. Nezamzadeh-Ejhih, Z. Banan, *Iran. J. Catal.* 2 (2012) 79-83.